Comparison of the 1D and 2D calculation models used for determination of the heat transfer coefficient during flow boiling heat transfer in a minichannel

Kinga Strąk[1*], *Magdalena* Piasecka[2], and *Beata* Maciejewska[3]

[1,2]Faculty of Mechatronics and Mechanical Engineering, Kielce University of Technology, Al. 1000-lecia P.P. 7, 25-314 Kielce, Poland
[3]Faculty of Management and Computer Modelling, Kielce University of Technology, Al. 1000-lecia P.P. 7, 25-314 Kielce, Poland

Abstract. The paper discusses the results of the flow boiling heat transfer in a vertical minichannel with rectangular cross-section. The heating element for FC-72 flowing in the minichannel is a thin plate. Infrared thermography is used to determine changes in the temperature on its outer side. The aim of the calculation is to determine the heat transfer coefficient using 1D and 2D calculation models. Local values of heat transfer coefficient on the surface between the heated plate and boiling fluid are calculated from the Newton`s and Fourier`s laws. In 2D model the plate temperature distribution is obtained by solving the inverse heat conduction problem. The governing equation is solved by means of two methods: the non-continuous Trefftz method and the Beck method. The results are presented as plate temperature and heat transfer coefficient calculated using 1D and 2D models as a function of the distance from the minichannel inlet. The analysis of the results revealed that the values and distributions of the heat transfer coefficient calculated by means of both models were similar. This suggests that all mentioned methods are interchangeable.

1 Introduction

The mechanism of heat transfer in minichannels is a complicated phenomenon not fully understood yet. With reduced dimensions of devices, it is possible to achieve an intensive flow boiling heat transfer in minichannels. The use of mini heat exchangers reduces both the size of the device and its costs, while the power of the device remains unchanged. An overview of the literature on heat transfer in minichannels can be found in the following works: [1-4]. The application of an enhancement of the heated plate surface may increase the intensity of heat transfer [5, 6]. In the literature, [7-10] the results of pool boiling heat transfer when the enhancement of the heated surface was applied in the form of mini-fins were described.

A lot of mathematical methods: analytical, analytical -numerical or numerical are applied for heat transfer calculation during flow boiling heat transfer in minigaps. Heat transfer coefficient computations using a one-dimensional model proposed by the authors were described in papers [11-14]. The 1D model assumes that heat flux conducted through the heated wall and absorbed by the fluid from the wall, at the contact surface of the heater - fluid flowing in the minichannel, are equal.

In paper [15] the results of studies of heat transfer and pressure drop during flow boiling of refrigerants are presented. The author proposed an analytical model of heat transfer and pressure drop by using of the experimental results.

The heat transfer coefficient in flow and pool boiling was calculated by using analytical method in articles [16-18].

The heat transfer issues can be modelled by numerically method using specialized software such as ANSYS CFX and Fluent like in [19, 20].

The two-dimensional calculation model was presented by the authors e.g. in [21, 22]. This model was proposed to identify the heat transfer coefficient at the flowing fluid-heated wall contact surface the wall temperature, the fluid temperature and the wall temperature gradient, by solving the inverse heat transfer problem [23]. One of the classical methods used to solve inverse problems is the sensitivity coefficient method (the Beck method) [22, 23]. This method consists in transforming the inverse problem into a few direct problems by differentiation the measured quantity with respect to the identified quantity. Inverse problems can also be solved by the method based on the functions that strictly satisfy the governing equation, so-called Trefftz functions [24-31]. The approximate solution of a differential equation, in form a linear combination of the Trefftz functions, is fitted to the given boundary conditions.

For the inverse heat transfer problem solving other methods as Hybrid Picard-Trefftz Method [32] and Fourier transform can be applied [33].

* Corresponding author: kzietala@tu.kielce.pl

2 Experiment

The principal aim of experiments was to collect data for analysing flow boiling heat transfer using the experimental stand shown in Fig. 1.

The main loops of the set-up are:

- the flow loop with the working fluid (Fluorinert FC-72, 3M),
- the data and image acquisition system consists of: an infrared camera (E60, FLIR), data acquisition stations, PC computer with appropriate software and the lighting system,
- the power supply system.

The accuracy of the IR camera is ± 1 °C or ± 1% in the temperature range 0 – 120 °C.

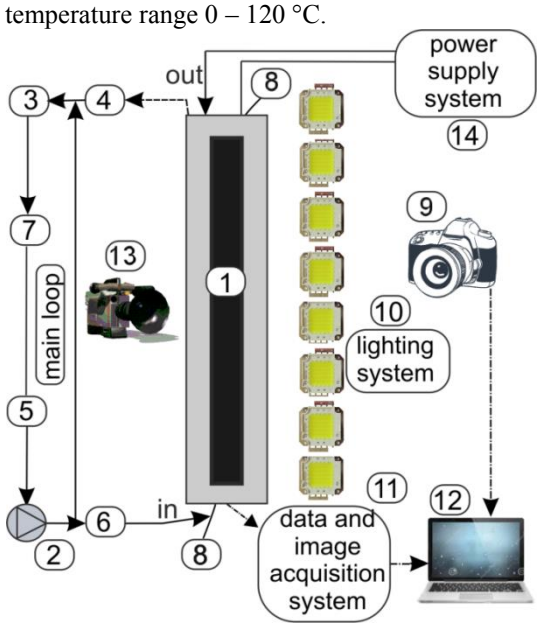

Fig. 1. The schematic diagram of the main systems of the experimental setup, 1-test section with a minichannel, 2-gear pump, 3-compensating tank/pressure regulator, 4-tube-type heat exchanger, 5-filters, 6- mass flowmeter, 7-deaerator, 8-pressure converter, 9-quick shot camera, 10- high power LEDs, 11-data acquisition station, 12-PC, 13-infrared camera, 14-power supply.

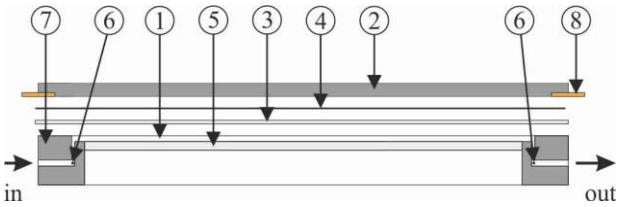

Fig. 2. Schematic diagram of the test section: 1-minichannel, 2-front cover, 3-PTFE spacer, 4-heated plate, 5-glass panel, 6-thermocouple, 7- channel body, 8-copper electrode.

The essential element of the main loop is a test section with a minichannel of 1.7 mm in depth, 16 mm in width and 180 mm in length (Fig. 2). The test section is vertically oriented with upward flow in a minichannel. The heated element being in contact with the fluid flowing in the minichannel is a smooth plate (*Ra* = 0.1752 μm [13]) made of Haynes-230 alloy, Haynes Int.), 0.45 mm thick. The properties of this alloy were given in [34].

The temperature of the heated plate was measured by infrared thermography (IRT), in the central, axially symmetric part of the minichannel. The outer surface of the plate was coated with black paint of known emissivity (about 0.97).

During the experimental series, the flow of the working fluid (FC-72) in the minichannel was laminar. When the desired values of the fluid pressure and flow rate were reached, there was a gradual increase in the electric power supplied to the heated plate followed by an increase in the heat flux transferred to the fluid in the minichannel.

3 Analysis and modelling

In this paper, local heat transfer coefficients were determined using the one-dimensional and two-dimensional models.

3.1. The one-dimensional model

Heat flow direction perpendicular to the direction of the fluid flow in the minichannel was taken into account. In the subcooled boiling region, the local heat transfer coefficients were determined from the following equation:

$$h_{1D}(x) = q''_{1D} / (T_{IRT}(x) - T_f(x) - q''_{1D}\frac{\delta}{k}) \quad (1)$$

where: x − distance from the minichannel inlet along the direction of the flow, T_{IRT} − plate temperature, measured by using infrared camera, T_f − fluid temperature calculated from the assumption of the linear distribution of the fluid temperature along the minichannel, k − thermal conductivity of the heated plate, δ − thickness of the heated plate, q''_{1D} − density of the heat flux transferred from the heated plate to the fluid, defined as:

$$q''_{1D} = (I\ \Delta U / A) - q''_{loss} \quad (2)$$

where: I − current, ΔU − voltage drop across the heated plate, A − surface area of the plate, q''_{loss} − heat loss to the surroundings.

The loss of heat to the surroundings was estimated according to formula:

$$q''_{loss} = h_s \quad [T_{IRT}(x) - T_s] \quad (3)$$

where h_s − local values of the heat transfer coefficient at the interface between the heated plate and the surroundings, T_s − ambient temperature.

3.2. The two-dimensional model

It was assumed that the heat flow through the main elements of the test section was steady-state and two-dimensional, and that there were no temperature changes along the minichannel width.

Local values of the heat transfer coefficient were calculated from Newton's law:

$$h_{2D}(x)=\frac{q''_{2D}(x,\delta)}{T_P(x,\delta)-T_f(x)} \tag{4}$$

where: q''_{2D} – density of the heat flux obtained in proposed 2D calculated methods, T_P – calculated plate temperature, δ and T_f defined as for Eq. (1).

The heat flux density q''_{2D} and the plate temperature T_P were determined by solving the inverse heat conduction problem in the heated plate:

$$\frac{\partial^2 T_P}{\partial x^2}+\frac{\partial^2 T_P}{\partial y^2}=\frac{I\,\Delta U}{A\,\delta\,k} \text{ for } (x,y)\in\Omega \tag{5}$$

where $\Omega=\{(x,y)\in R^2: 0<x<L,\quad 0<y<\delta\}$, L – length of the minichannel, δ, k, $I, \Delta U$, A defined as for Eqs. (1) and (2), respectively. The boundary conditions are shown in Fig. 3.

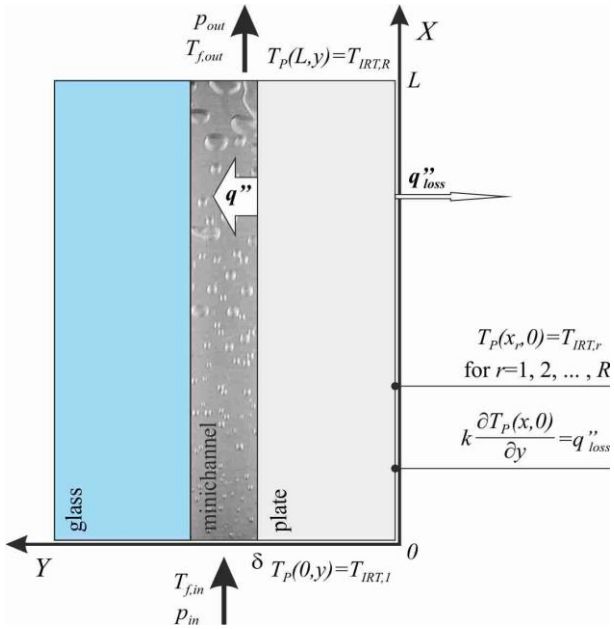

Fig. 3. Boundary conditions.

The inverse problem (no boundary condition at $y=\delta$ boundary) was solved using two methods: the non-continuous Trefftz method and the Beck method.

3.2.1 The non-continuous Trefftz method

The plate temperature in each of subdomains $\Omega_j=\{(x,y)\in R^2: x_{j-1}\le x\le x_j,\quad 0\le y\le\delta\}$, for $j=1,2,....,J$, where $\Omega=\bigcup_{j=1}^{J}\Omega_j$ was a linear combination of the Trefftz functions:

$$T_{P,j}(x,y)=u(x,y)+\sum_{i=1}^{N}a_{ij}v_i(x,y) \tag{6}$$

where: $u(x,y)$ – particular solution of Eq. (5), and $v_i(x,y)$ – Trefftz functions.

The coefficients a_{ij} minimize the functional which expresses the mean square error of the approximate solution on the boundary and on the common edges of the neighbouring subdomains [35].
The heat flux from Eq. (4) was obtained according to the Fourier law:

$$q''_{2D}(x,\delta)=-k\frac{\partial T_P(x,\delta)}{\partial y} \tag{7}$$

3.2.2 The Beck method

The plate temperature T_P dependent on the constant heat fluxes q''_m for $m=1,2,\ldots,M$ at the boundary $y=\delta$ for $0\le x\le L$, like in [37], is expanded into a Taylor series around the point $(q''_{01},\ldots,q''_{0M})$. Since higher order derivatives vanish in linear problems, the formula has the form:

$$T_P(x,y,q''_1,\ldots,q''_M)=\Theta(x,y)+\sum_{m=1}^{M}Z_m(x,y)(q''_m-q''_{0m}) \tag{8}$$

where $\Theta(x,y)=T_P(x,y,q''_{01},\ldots,q''_{0M})$, while the sensitivity coefficients $Z_m(x,y)$, for $m=1,2,\ldots,M$ are defined:

$$Z_m(x,y)=\left.\frac{\partial T_P}{\partial q_m}\right|_{q''_m=q''_{0m}} \tag{9}$$

The functions $\Theta(x,y)$ and $Z_m(x,y)$ for $m=1,2,\ldots M$ in the domain Ω were the solution of the $1+M$ direct problems obtained after substituting Eq. (8) into Eq. (5) and to the boundary conditions given in Fig. 3.

The direct problems were solved by means of the Trefftz method [36].

The values of q''_m for $m=1,2,\ldots M$ in Eq. (8) were calculated, like in [21], as the minimum of the functional:

$$F=\sum_{r=1}^{R}\left(T_P(x_r,y_r,q''_1,\ldots,q''_M)-T_{IRT,r}\right)^2 \tag{10}$$

3 Results and discussion

This paper shows the results of heat transfer during fluid flow in a vertically oriented minichannel at the subcooled boiling region. The experiments involved increasing the heat flux supplied to the heated plate. The outer plate surface temperature was measured using an infrared camera. The experiments were conducted under steady-state conditions.

In the experiment, the heat transfer between the heated plate surface and fluid FC-72 in the minichannel was initially by single phase convection. When the heat flux supplied to the heated plate was increased, the boiling initiation occurred. In the subcooled boiling region the liquid became superheated only in the vicinity of the heated plate surface while in the core of the flow, it was highly subcooled.

Data from several experimental series were analysed when three values of heat flux supplied to the heated plate and three values of fluid pressure at the inlet were set. The heat transfer coefficient was calculated using 1D and 2D calculation models. Local values of the coefficient in the contact surface between the heated plate and working fluid were determined from the Newton`s and Fourier`s laws. In 2D model the plate temperature distribution was obtained by solving the inverse heat conduction problem. The governing equation was solved by means of the non-continuous Trefftz method and the Beck method.

The results are presented as:

- the plate temperature vs .the distance from the minichannel inlet (Fig. 4),
- the heat transfer coefficient as a function of the distance from the minichannel inlet, calculated using 1D and 2D models, at three values of inlet pressure: 130 kPa, 150 kPa, 165 kPa (Fig. 5),
- the heat transfer coefficient vs. the distance from the minichannel inlet, calculated according to 1D and 2D models on the basis of experimental data obtained at three values of heat flux: 54 kW/m^2, 66 kW/m^2 and 82 kW/m^2 (Fig. 6).

Experimental parameters are shown in Table 1.

Table. 1. Experimental parameters.

Heat flux q''_{1D} kW/m^2	Average mass flux G kg /(m^2·s)	Average inlet pressure p_{in} kPa	Average inlet liquid subcooling ΔT_{sub} K
54	411	130	47
		150	
		165	
66	421	130	51
		150	
		165	
82	427	130	54
		150	
		165	

The temperature distributions on the heated plate surface, illustrated in Fig. 4, indicate that the highest plate temperature was achieved at lower inlet pressure of 130 kPa and the highest heat flux of 82 kW/m^2 (Fig. 4a). At the highest value of inlet pressure (165 kPa) and the lowest value of heat flux (54 kW/m^2), the lowest temperature of the heated plate was obtained from measurements (Fig. 4c).

When analyzing the results illustrated in Figs. 5 and 6 it can be noticed that there was an increase in the local values of the heat transfer coefficient with an increase in the distance from the minichannel inlet. The local values of the heat transfer coefficient obtained from 1D model were higher in comparison to determined according to 2D model with using the Beck and the non-continuous Trefftz methods at three values of inlet pressure (Fig. 5) and three values of heat flux (Fig. 6).

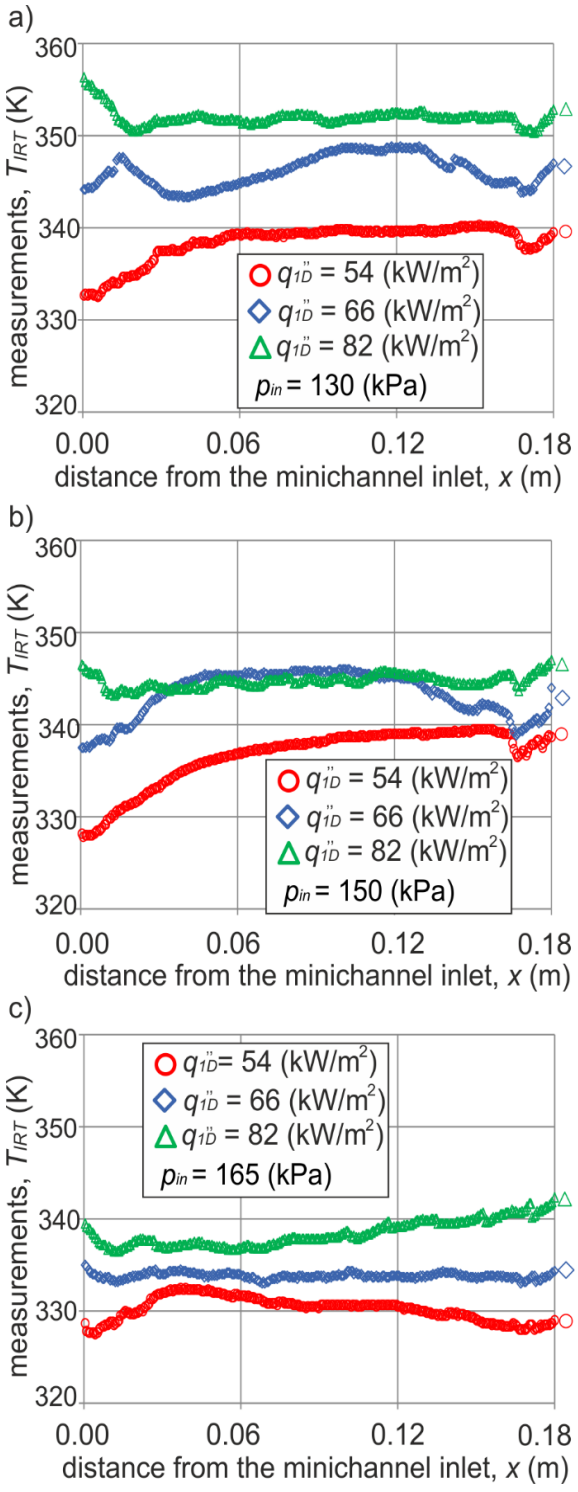

Fig. 4. The plate temperature measured by infrared thermography vs. the distance from the minichannel inlet, at selected values of heat flux and inlet pressure, experimental parameters shown in Table 1.

The relative differences between the values of the heat transfer coefficients obtained for 1D and 2D models were calculated according to the following formula:

$$\sigma_i = \frac{1}{R}\sum_{r=1}^{R}\sqrt{\frac{\left(h_{1D}(x_r) - h_{2D,i}(x_r)\right)^2}{\left(h_{1D}(x_r)\right)^2}} \quad \text{for } i = \text{NCT, B} \quad (11)$$

where NCT and B denote the results from application the non-continuous Trefftz method and the Beck method, respectively, R - the number of measurements, h_{1D} and h_{2D} are the values of the heat transfer coefficients calculated by means of 1D and 2D models.

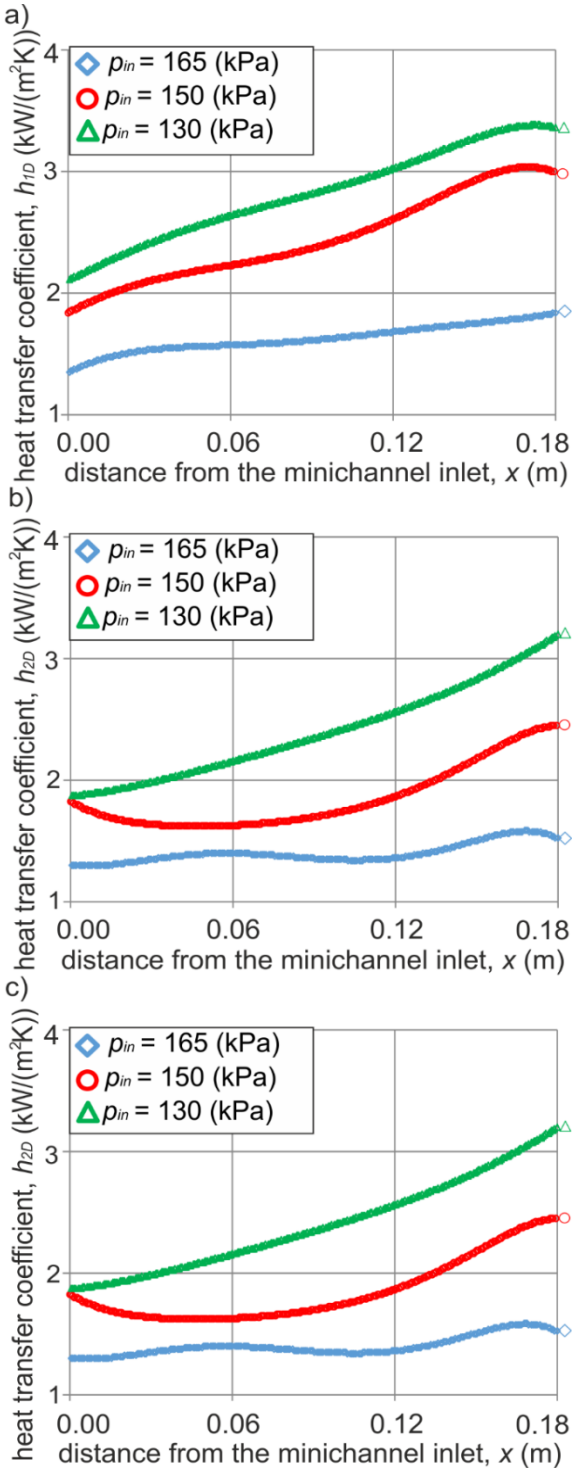

Fig. 5. The heat transfer coefficient vs. the distance from the minichannel inlet, calculated according to: 1D model (a) and 2D model (b,c) using: the Beck method (b) or the non-continuous Trefftz method (c),at heat flux of 82 kW/m^2 and selected inlet pressure; experimental parameters shown in Table 1.

The analysis of the results revealed that the values and distributions of the heat transfer coefficient calculated by means of 1D model and 2D model using the Beck and the non-continuous Trefftz methods, were similar at the same heat flux supplied to the heated plate.

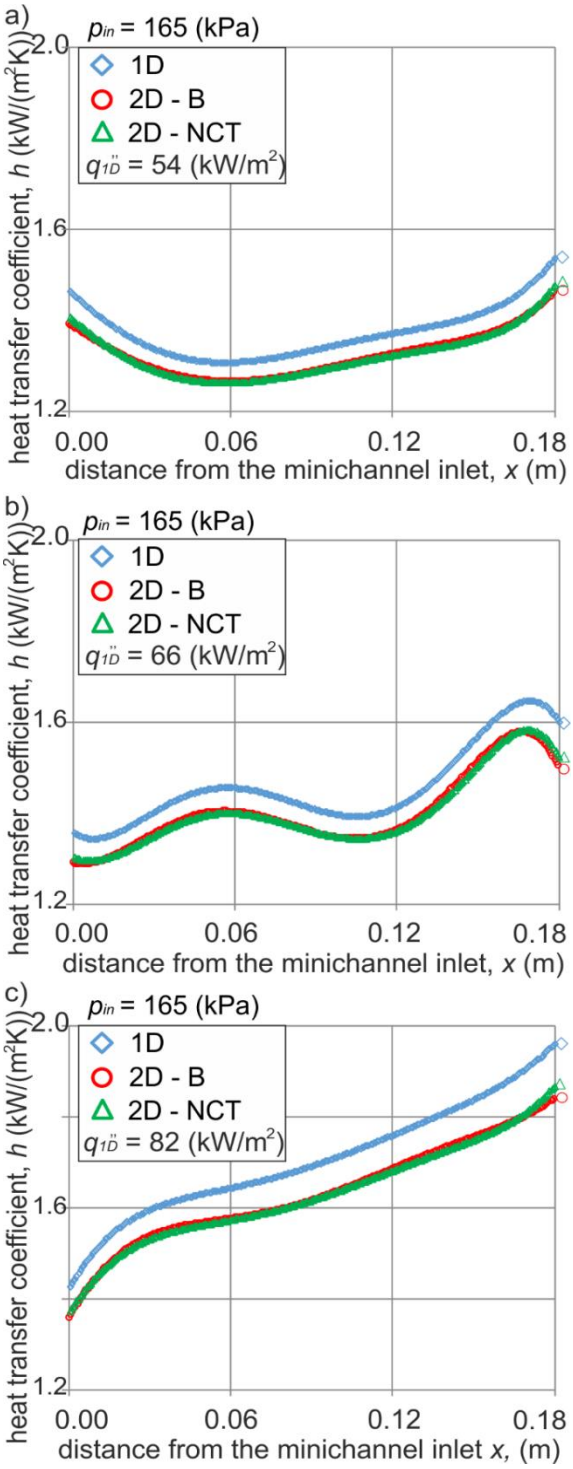

Fig. 6. The heat transfer coefficient vs. the distance from the minichannel inlet calculated according to 1D and 2D models with using: the Beck method (B) and the non-continuous Trefftz method (NTC),at the same value of inlet pressure, experimental parameters shown in Table 1.

The obtained relative differences from above calculations are shown in Table 2.

Table. 2. Relative differences between heat transfer coefficient values calculated using1D model and 2D model with using the Beck and the non-continuous Trefftz methods.

Average inlet pressure p_{in} kPa	Heat flux q''_{1D} kW/m^2	Beck method σ %	Non-continuous Trefftz method σ %
130	54	3.7	3.6
	66	3.9	3.8
	82	4.5	4.4
150	54	4.3	4.2
	66	5.2	5.0
	82	6.8	6.6
165	54	5.5	5.4
	66	6.7	6.5
	82	7.9	7.7

3 Conclusions

This paper has compared the results calculated according to proposed one-dimensional calculation model and two-dimensional one with application of two methods: the non-continuous Trefftz method and the Beck method. The proposed models were applied to solve the two-dimensional inverse heat transfer problem during FC-72 flow in a vertical minichannel of rectangular cross-section. The aim of the calculation was to determine the heat transfer coefficient on the basis of the heated wall temperature measured by infrared thermography on the outer heater's surface. The results were presented as local plate temperatures and heat transfer coefficients calculated using 1D and 2D models and above mentioned methods. The temperature distributions on the heated plate surface indicate that the highest plate temperature was achieved at lowest inlet pressure and the highest heat flux. At the highest value of inlet pressure and the lowest value of heat flux, the lowest temperature of the heated plate was obtained from measurements. There was an increase in the local values of the heat transfer coefficient with an increase in the distance from the minichannel inlet. The heat transfer coefficient values obtained from 1D model were higher in comparison to determined according to 2D model. The relative differences in the coefficients calculated using both models were low. The analysis of the results revealed that the values and distributions of the heat transfer coefficient calculated by means of proposed calculation models and methods were similar. This suggests that all mentioned methods are interchangeable.

The research reported herein was supported by a grant from the National Science Centre, Poland (No. DEC-2016/23/N/ST8/01247).

References

1. R. Charnay, J. Bonjour, R. Revellin, Int. J. Heat Fluid Flow **46**, 1–16 (2014)
2. K. H. Bang, K. K. Kim, S. K Lee B., W. Lee, Int. J. Therm. Sci. **50**(3), 280–286 (2011)
3. K. Strąk, M. Piasecka, B. Maciejewska, Int. J. Heat Mass Transf. **117**, 375–387 (2018)
4. K. Strąk, M. Piasecka, E3S Web Conf. **70**, 02014 (2018)
5. Ł.J. Orman, N. Radek, A. Kapjor, Mater. Res. Proc. **5**, 216–219 (2018)
6. Ł.J. Orman, N. Radek, J. Bronček, Mater. Res. Proc. **5**, 189–193 (2018)
7. R. Kaniowski, R. Pastuszko, EPJ Web Conf. **180**, 02042 (2018)
8. R. Kaniowski, R. Pastuszko, Ł. Nowakowski, EPJ Web Conf. **143**, 02049 (2017)
9. R. Kaniowski, R. Pastuszko, EPJ Web Conf. **25**, 02019 (2012)
10. R. Pastuszko, Int. J. Therm. Sci. **125**, 197–209 (2018)
11. K. Strąk, M. Piasecka, Trans. Inst. Fuid-Flow Mach. **128**, 97–118 (2015)
12. M. Piasecka, K. Strąk, B. Maciejewska, Heat Transf. Eng. **38**, 332–346 (2017)
13. K. Strąk, M. Piasecka, EPJ Web Conf. **180**, 02098 (2018)
14. M. Piasecka, K. Strąk, Heat Transf. Eng. **40** (13-14), 1162-1175 (2019)
15. T. Bohdal, Int. J. Heat Fluid Flow **21**, 449–455 (2000)
16. M. C. Díaz, J. Schmidt, Int. J. Heat Fluid Flow, **28**(1), 95–102 (2007)
17. J. T. Cieśliński, K. Krasowski, J. Enhanc. Heat Transf. **20**, 165–177 (2013)
18. A. A. Chehade, H. Louahlia, S. Le Masson, F. Fardoun, A. Besq, Nanoscale Res. Lett. **8**(1), 130 (2013)
19. B. Maciejewska, S. Błasiak, M. Piasecka, EPJ Web Conf. **143**, 02071 (2017)
20. A. Diani, K .K. Bodla, L. Rossetto, S. Garimella, Int. J. Heat Mass Transf. **88**, 508–515 (2015)
21. B. Maciejewska, K. Strak, M. Piasecka, Int. J. Numer. Methods Heat Fluid Flow **28**, 206–219 (2018)
22. B. Maciejewska, J. Theor. Appl. Mech. **55**, 103–116 (2017)
23. J. V. Beck, B. Blackwell, C. R. St. Clair, *Inverse heat conduction. Ill-posed Problems* (Wiley - Interscience Publ., New York, 1985)
24. E. Trefftz, Proc. Int. Kongress für Technische Mechanik, Zürich, 131-137 (1926)
25. B. Maciejewska, M. Piasecka, Int. J. Numer. Methods Heat Fluid Flow, doi:10.1108/HFF-12-2018-0781 (2019)
26. M. J. Ciałkowski, J. Therm. Sci. **11**, 148–162 (2002)
27. K. Grysa, B. Maciejewska, J. Theor. Appl. Mech. **51**, 251-264 (2013)

28. A. Maciąg, A. Pawinska, Comput. Appl. Math. **35**, 187–201 (2016)
29. S. Hożejowska, J. Theor. Appl. Mech. **53**, 969–980. 2015
30. K. Grysa, A. Maciag, A. Cebo-Rudnicka, M. Walaszczyk, Engineering Analysis with Boundary Elements **95**, 33–39 (2018)
31. S. Blasiak, A. Pawinska, Int. J. Heat Mass Transf. **90**, 710–718 (2015)
32. M. Grabowski, S. Hozejowska, A. Pawinska, et al., Energies **11**(8), 2057 (2018)
33. A. Wroblewska, A. Frackowiak, M. Cialkowski, Inverse Probl. Sci. En. **24**(2), 195-212 (2016)
34. http://www.haynesintl.com
35. B. Maciejewska, M. Piasecka, Heat Mass Transf. **53**, 1211–1224 (2016)
36. B. Maciejewska, K. Strąk, M. Piasecka, EPJ Web Conf. **114**, 02068 (2016)
37. B. Kruk, M Sokała, J. Appl. Math. Mech. **3**, 693–694 (1999)